RESEARCH ARTICLE

Basaltic ignimbrites in monogenetic volcanism: the example of La Garrotxa volcanic field

J. Martí[1,2] · L. l. Planagumà[3] · A. Geyer[1] · G. Aguirre-Díaz[4] · D. Pedrazzi[3] · X. Bolós[5]

Abstract Ignimbrites are pyroclastic density current deposits common in explosive volcanism involving intermediate and silicic magmas and in less abundance in eruptions of basaltic central and shield volcanoes. However, they are not widely described in association with monogenetic volcanism, where typical products include lava flows, scoria and lapilli fall deposits, as well as various kinds of pyroclastic density current deposits and explosion breccias. In La Garrotxa basaltic monogenetic volcanic field, part of the Neogene-Quaternary European rift system located in the northeast of the Iberian Peninsula, we have identified a particular group of pyroclastic density current deposits that show similar textural characteristics to silicic ignimbrites, indicating an overlap in transport and depositional processes. These deposits can be clearly distinguished from other pyroclastic density current deposits generated during phreatomagmatic phases that typically correspond to thinly laminated units with planar-to-cross-bedded stratification. The monogenetic ignimbrite deposits correspond to a few meters to several tens of meters thick units rich in lithic- and lapilli scoria fragments, with an abundant ash matrix, and internally massive structure, emplaced along valleys and gullies, with run-out distances up to 6 km and individual volumes ranging from 10^6 to 1.5×10^7 m^3. The presence of flattened scoria and columnar jointing in some of these deposits suggests relatively high emplacement temperatures, coinciding with available paleomagnetic data that suggests an emplacement temperature around 450–500 °C. In this work, we describe the main characteristics of these pyroclastic deposits that were generated by a number of phreatomagmatic episodes. Comparison with similar deposits from silicic eruptions and previous examples of ignimbrites associated with basaltic volcanism allows us to classify them as 'basaltic ignimbrites'. The recognition in monogenetic volcanism of such pyroclastic products, which may extend several kilometres from source, has an important consequence for hazard assessment in these volcanic fields, which previously have been considered to present only minor hazards and risks.

Keywords Basaltic ignimbrites · Monogenetic volcanism · La Garrotxa volcanic field · Volcanic hazards

✉ J. Martí
  joan.marti@ictja.csic.es

1 Group of Volcanology, Institute of Earth Sciences "Jaume Almera", CSIC, Lluís Solé Sabaris s/n, 08028 Barcelona, Spain

2 Present address: Institut des Sciences de la Terre d'Orleans (ISTO, CNRS), Université d'Orleans, Campus Géosciences, 1A rue de la Férolerie, F45071 Orleans Cedex 2, France

3 Tosca Environmental Services. La Garrotxa Volcanic Zone Natural Park, 17800 Olot, Spain

4 Centro de Geociencias, UNAM, Campus de Juriquilla, 76230 Queretaro, Mexico

5 Institute of Geophysics, UNAM, Campus Morelia, 58190 Morelia, Michoacán, Mexico

Introduction

Pyroclastic density currents (PDCs) are high-speed, gravity-driven flows of hot particles (magma and rock fragments) and gas (Druitt 1998; Burgisser and Bergantz 2002; Sulpizio and Dellino 2008; Dufek et al. 2015; Dufek 2016) that represent one of the main hazards associated with explosive volcanism (Blong 1984, 2000; Tilling 1989, 2005). They range from expanded, turbulent suspension currents formed by lateral blasts or by the fountaining of vertical eruption columns, to highly concentrated granular avalanches formed after lava

dome collapse or as dense underflows beneath suspension currents (Druitt 1998). In a similar way to what is used in sedimentology to distinguish among different types of sediment gravity flows (e.g. Middleton and Hampton 1973; Middleton 1993; Lowe 1979, 1982), the current tendency in volcanology is to consider the different typologies of PDCs within a continuum that spans from very dilute (fluid-dominated) to highly concentrated (solid-dominated) flows (e.g. Branney and Kokelaar 2002; Sulpizio and Dellino 2008). This has improved understanding of the shared features of former end members such as pyroclastic flows (high particle concentration) and pyroclastic surges (low particle concentration) and the deposits they generate and has led to their interpretation in terms of fluid dynamics rather than eruption characteristics. Ignimbrites are generated by the emplacement of high particle concentration PDCs that are rich in pumice fragments (Sparks et al. 1973) and have traditionally been considered as a common product of explosive volcanism involving intermediate and silicic magmas. They are generally associated with collapsing vertical eruption columns and form dense pyroclastic density currents of variable temperature that tend to emplace preferentially into topographic lows but can also cover topographic highs given their great momentum (Sparks et al. 1978; Wilson et al. 1980). Ignimbrite deposits are typically poorly sorted mixtures of volcanic ash (glass shards and crystal fragments) and pumice and lithic lapilli and range from unconsolidated to densely welded depending on the temperature of emplacement. These deposits may range in volume from 10^3 to $> 10^{12}$ m^3 depending on the magnitude of the eruption. Such type of PDCs have been inferred to have emplaced either en masse (Sparks 1976) or by progressive aggradation (Branney and Kokelaar 1992). Due to their high velocity of emplacement, temperature, dynamic pressure and their long-runout distances, they represent a major hazard during explosive volcanic eruptions (Blong 1984, 2000; Tilling 1989, 2005). This type of pyroclastic deposit is infrequently described from eruptions of composite basaltic volcanoes (Freundt et al. 2000), as is rarely reported in the deposits of monogenetic basaltic volcanism (White 1991; White and Schmincke 1999; Giordano et al. 2002; van Otterloo et al. 2013; van Otterloo and Cas 2016), which is typically characterised by the presence of lava flows, scoria and ash fall deposits, as well as different kinds of PDCs and explosion breccias, when it becomes phreatomagmatic in character (Wohletz and Sheridan 1983; Walker 2000; Valentine and Gregg 2008).
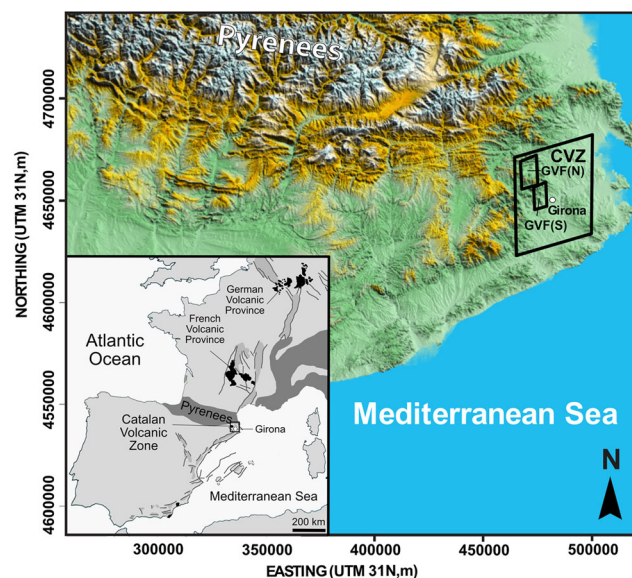
In La Garrotxa volcanic field (GVF) (Martí et al. 2011; Bolós et al. 2015), we have identified a particular group of massive pyroclastic density current deposits with similar lithological and sedimentological characteristics to those of silicic ignimbrites, which suggests similar transport and depositional mechanisms were in operation. They are lithologically and sedimentologically different to the deposits of dilute PDCs

that were generated by phreatomagmatic explosions in the volcanic field (see Martí et al. 2011). We here describe their stratigraphy, lithology and sedimentological features and interpret their eruptive, transport and depositional mechanisms. We go on to compare them with similar deposits generated by explosive silicic volcanism and conclude that these PDC deposits, generated by basaltic monogenetic volcanism, share many characteristics with silicic ignimbrites.

Geological setting

The GVF is part of the Catalan Volcanic Zone (NE Spain), one of the Quaternary alkaline volcanic provinces associated with the intraplate European Cenozoic Rift System (Martí et al. 1992) (Fig. 1). It covers an area of about 600 km^2 and is located between the cities of Olot and Girona (Fig. 1). It contains >50 monogenetic basaltic volcanoes including cinder cones, tuff rings and maars that range in age from 0.7 Ma to early Holocene (Martí et al. 2011; Bolós et al. 2014). Upper Palaeozoic, Eocene and Quaternary crustal rocks form the substrate. The GVF embraces two geographically distinct zones, one in the north of the county of La Garrotxa that contains most of the volcanoes and a second a smaller area to the south that contains fewer, but larger and more complex, volcanic edifices (see Bolós et al. 2014, Fig. 1).

Volcanism in the GVF was fed by basaltic and basanitic magmas (Araña et al. 1983; Cebriá et al. 2000). A notable feature is the presence of mantle xenoliths and lower crust cumulates (Araña et al. 1983; López Ruiz and Rodriguez

Fig. 1 Map of the study area. **a** Distribution of the European Cenozoic Rifts System. **b** Location of the Catalan Volcanic Zone (CVZ) and La Garrotxa Volcanic Field (GVF) (N and S in *squares* indicate the northern and southern sectors of the GVF, respectively)

Badiola 1985; Martí et al. 1992; Neumann et al. 1999; Cebriá et al. 2000), which suggests that the magmas were sourced from considerable depth (Bolós et al. 2015).

Volcanic activity in the GVF is characterised by numerous small cinder cones built during short-lived monogenetic eruptions along tectonic-related volcanic fissures. The total volume of extruded magma in each eruption was between 0.01 and 0.2 km^3 dense rock equivalent (DRE). Strombolian and phreatomagmatic episodes alternated in most of these eruptions and have given rise to complex stratigraphic sequences composed of a broad range of types of pyroclastic deposits (Martí and Mallarach 1987; Gisbert et al. 2009; Martí et al. 2011; Cimarelli et al. 2013; Bolós et al. 2014). The eruption sequences differ from one cone to another, demonstrating that the eruptions did not follow a common pattern, particularly in cases where magma and water interacted. This complex eruptive behaviour may be related to the differing stratigraphic, structural and hydrogeological characteristics of the substrate below each volcano rather than to any differences in the physics or chemistry of the erupting magmas, which were generally fairly homogeneous throughout the lifetime of GVF (Martí et al. 2011; Bolós et al. 2014, 2015).

Description of the massive PDC deposits in the GVF

The monogenetic volcanism of the Catalan Volcanic Zone has produced a wide spectrum of deposits from most eruption styles of basaltic Strombolian and phreatomagmatic volcanism (Martí et al. 2011; Bolós et al. 2014), i.e. lapilli and scoria fallout deposits, ballistic bombs and spatter, explosion breccias, ash fallout and different types of PDC deposits. Among the PDC deposits, there are several massive units that have abundant lithic lapilli and scoria lapilli and abundant ash matrix, are internally massive and are a few meters to several tens of meters thick. These were emplaced along valleys and gullies, up to 6 km from source. The volumes of these deposits range from 10^6 to 1.5×10^7 m^3. These deposits can be clearly distinguished from more widespread, lithic-rich, thinly laminated units (typically a few centimetres to a few metres thick) with planar-to-cross-bedded stratification, which are interpreted as the deposits of dilute PDCs generated during phreatomagmatic phases (Martí et al. 2011; Pedrazzi et al. 2014, Pedrazzi et al. 2016; Bolós et al. 2014). Stratigraphic relationships demonstrate that the massive and thinly laminated PDC deposits correspond to two different types of deposits formed during different phases of the eruptions, rather than different lithofacies of a deposit that was strongly influenced by topography (cf. Wilson and Walker 1982; Cas and Wright 1987). The massive deposits, which constitute the main objective of this study, show characteristics that resemble ignimbrites associated with silicic volcanism, in particular with those of classical ignimbrites (e.g. Sparks et al. 1973). They

are also similar to deposits found in other monogenetic basaltic fields (White 1991; Giordano et al. 2002; van Otterloo et al. 2013; van Otterloo and Cas 2016). Deposits with these characteristics have been observed in several volcanoes in the GVF (see Martí and Mallarach 1987; Gisbert et al. 2009; Martí et al. 2011; Bolós et al. 2014). In the rest of this section, we describe the main characteristics of three of the most representative massive PDC deposits in the GVF.

Can Tià maar section

The Can Tià volcano is a maar-type edifice with a flat-bottomed, 270-m-wide and 20-m-deep crater (Martí et al. 2011). The stratigraphic sequence at this volcano (point 1, Fig. 2) is composed entirely of pyroclastic deposits and includes four main units from base to top (Fig. Fig. 3). The lower unit corresponds to a 10-cm-thick deposit of small (<1 cm) juvenile and lithic clasts in an ash matrix. This rests unconformably on a palaeosoil developed over Eocene sediments. The second unit is a ~6-m-thick Strombolian fall deposit, composed in its lower part of well-stratified, fine-grained, highly vesiculated scoria lapilli and bombs, which progressively grades into a poorly stratified to massive, coarse lapilli, non-welded scoria fall deposit. Towards the top, it becomes a thinly laminated, well-sorted, finer-grained and is rich in red Eocene sandstone lapilli and blocks (<2–30 cm). The third unit is only a few centimetres thick and has a well-stratified ash layer in its upper part. The upper unit has planar contact with the underlying scoria lapilli and ash layers and is a massive PDC deposit, up to 3 m thick, which contains abundant centimetric-to-decimetric Eocene lithic lapilli and blocks as well as dense-to-highly vesicular scoria lapilli fragments, surrounded by a lithic-rich, ash matrix that has been mostly altered to clay minerals, zeolites and iron oxides (Martí et al. 2011). At the base of the massive unit, there is a few centimetres thick fine-grained horizon that grades into a lithic-rich zone with coarse-tail grading of lithic clasts in the uppermost part of the deposit and in which scoria fragments become more abundant.

According to Martí et al. (2011), the succession of deposits observed in this volcano reveals that the explosive activity began with a short explosive event, probably of phreatomagmatic nature given the composition of the resulting deposits. Then, the eruption immediately changed to magmatic (second unit) and back to phreatomagmatic (third unit and fourth units). The succession of deposits and the distribution of lithic clasts reveal that the initial change in the eruptive behaviour (from phreatomagmatic to magmatic) was abrupt but that the second change (from magmatic to phreatomagmatic) was gradual, as indicated by the increasing content of Eocene lithic clasts towards the top of the second unit.

Fig. 2 Location and simplified geological maps of the studied deposits. *1* Can Tià. *2* Riu Els Arcs (proximal facies). *3* Riu Els Arcs (distal facies). *4* Riera de Canet d'Adri (proximal facies). *5* Riera de Canet d'Adri, Molí de Can Cadamont (distal facies)
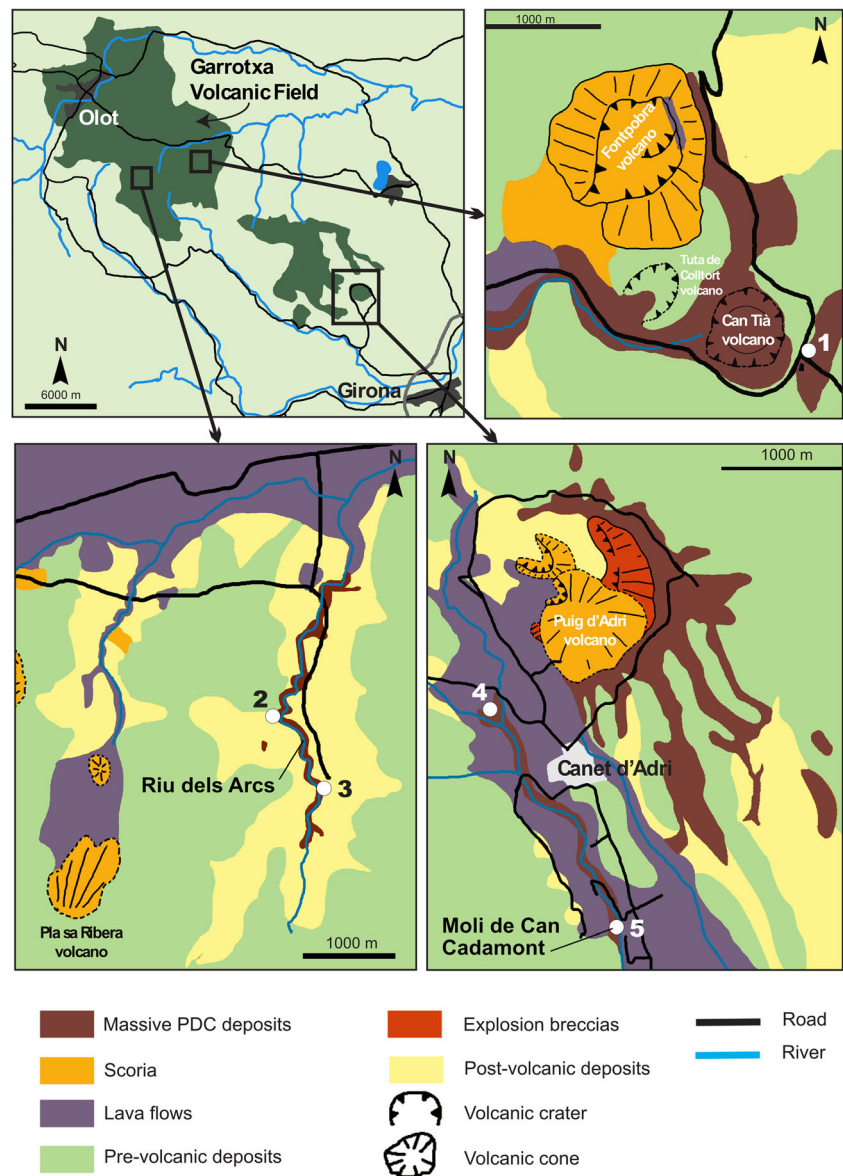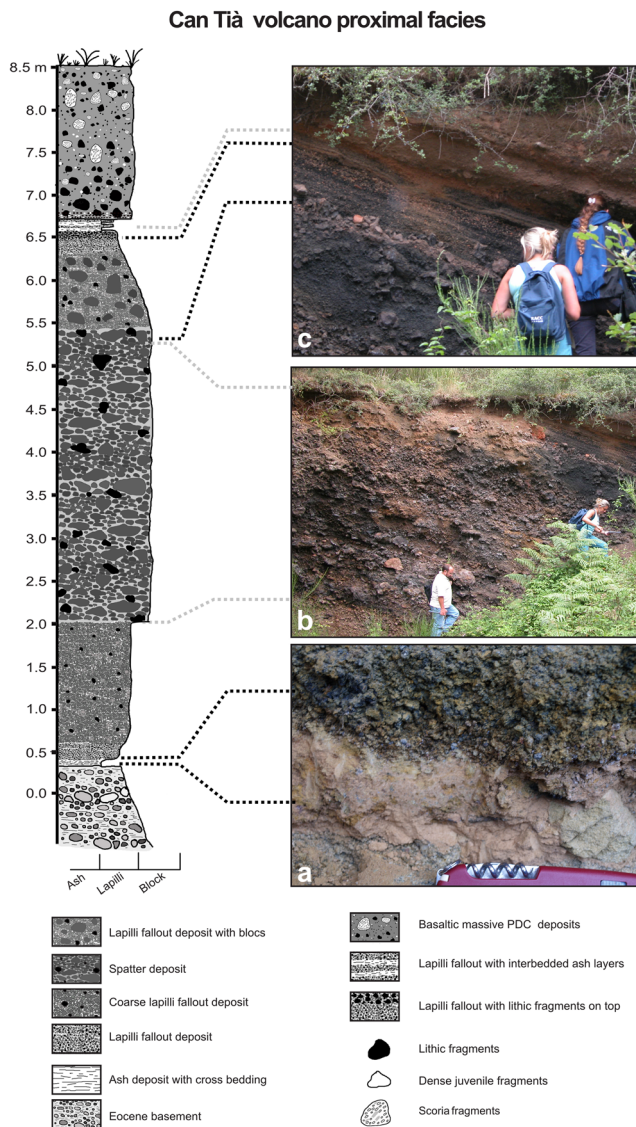
Riu Els Arcs sections

The Riu Les Arcs pyroclastic sequence (Fig. 2), thought to have been erupted by the Sant Jordi volcano, appears in the northern sector of the GVF (Fig. 1) and overlies Quaternary travertine in proximal areas and gravels and other fluvial deposits that infilled part of the same gully in more distal areas. There are two main units with different lithofacies depending on the distance from the vent (points 2 and 3, Fig. 2). At distances of ~1.5 km from the vent (Riu El Arcs, Fig. Fig. 4), the lower unit hugs the irregular pre-existing topography along the bottom of the gully and corresponds to a fine scoria lapilli fall deposit. It is well sorted and thinly laminated and mostly composed of highly vesicular, juvenile basaltic scoria clasts. The total thickness of this deposit is about 25 cm. Further from the vent (~ 3–4 km), this fallout
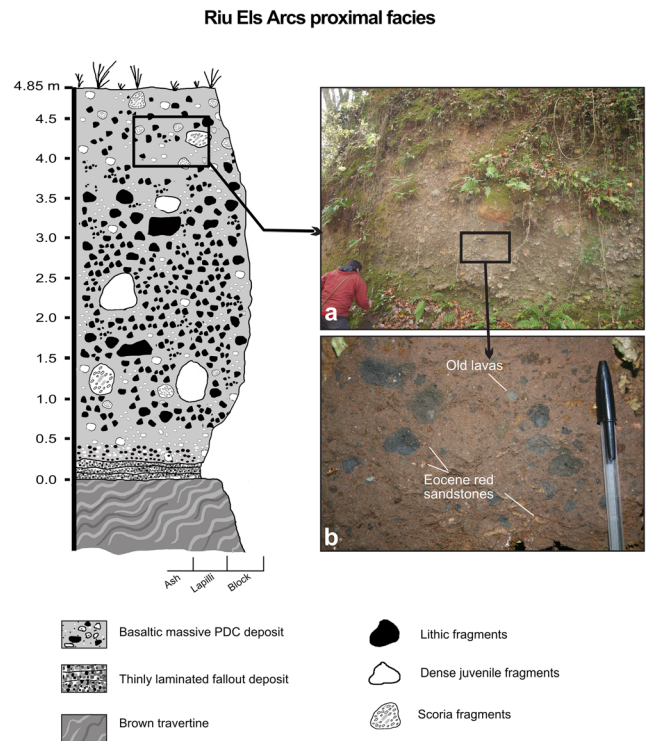
deposit maintains the same characteristics but is fine-grained. In distal areas (Fig. Fig. 5), it is preceded and overlain by a thinly laminated deposit, with cross bedding, which is composed of ash-sized juvenile and lithic fragments. These two dilute PDC deposits show a very irregular distribution and only appear in some outcrops. The lower layer clearly precedes the emplacement of the fallout deposit but seems to have been deposited irregularly because the fallout deposit locally overlies the substrate. The upper dilute PDC deposit only appears at medium-to-distal distances and in some places has been partially or totally eroded away by the emplacement of the upper unit.

The upper unit consists of a brown, massive, 15-m-thick PDC deposit composed of dense-to-highly vesiculated, large lapilli-to-bomb-sized juvenile scoria fragments that are sometimes flattened, together with lithic lapilli and blocks of

Can Tià volcano proximal facies


Riu Els Arcs proximal facies

Fig. 4 Riu dels Arcs proximal stratigraphic succession (see Fig. 2 point 2 for location) (UTM 31N—ETRS89 465911.3 and 4664588.1). **a** View of the upper part the massive PDC deposit. **b** close-up view of the massive PDC deposits in which juvenile scoria fragments (*black*) and lithic fragments of Eocene red sandstones (*red*) and old lavas (*grey*) can be observed

Fig. 3 Can Tià volcano stratigraphic succession (UTM 31N—ETRS89 462474.8 and 4663385.3). **a** Lower ash layer overlying the Eocene basement and covered by a well-sorted lapilli scoria deposit. **b** Lithic-rich scoria deposit. **c** Transition from the Strombolian lapilli scoria deposit into the phreatomagmatic units, composed at the base of alternating fine ash and fine lapilli scoria deposits and on top by a massive unit (massive PDC deposit) (layers 2a and 2b)

Eocene sedimentary rocks and previous lavas, matrix-supported in an indurated ash and fine lapilli matrix. Juvenile fragments contain plagioclase phenocrysts and distinctive megacrysts (1–2 cm in diameter) of olivine and plagioclase. This deposit is not homogeneous in either grain size, the distribution of components or in its internal stratification, and exhibits marked variations in lithofacies from proximal to distal areas. At proximal distances (Fig. Fig. 4), the base of the upper unit is mostly planar. Basal parts (the lowermost 0.2 m) are characterised by the presence of a fine ash layer that contains juvenile and lithic components. This fine-grained layer gradually grades into a lithic-rich horizon, about 0.4 m thick,

composed of dense fragments of Eocene sediments and older lavas up to 50 cm in diameter that are irregularly distributed from clast-supported and matrix-supported zones. In the rest of the deposit, the lithic content varies vertically and can form lithic-rich zones or lenses. Juvenile clasts are also irregularly distributed through the deposit but tend to be concentrated towards the top. They range from equant to flattened. The matrix of this massive unit is relatively coarse to fine-grained and is composed of devitrified glass shards, small scoria fragments and lithic clasts, cemented by zeolites, carbonate and iron oxides (mainly hematite) that fill the inter-clast porosity and the vesicles of the juvenile clasts. In some places, carbonate cement has partially replaced the original volcanic glass, which has been mostly altered into clay minerals. The top of the deposit has been partially eroded, reworked and transformed into a palaeosoil.

### Puig d'Adri volcano sections

As in the Riu dels Arcs massive deposit, at Puig d'Adri (Fig. 2), there are significant variations in the lithofacies from proximal to distal locations. This massive PDC deposit is only exposed along the Canet d'Adri river, where it forms a continuous outcrop over 5 km in length. It has been channelized
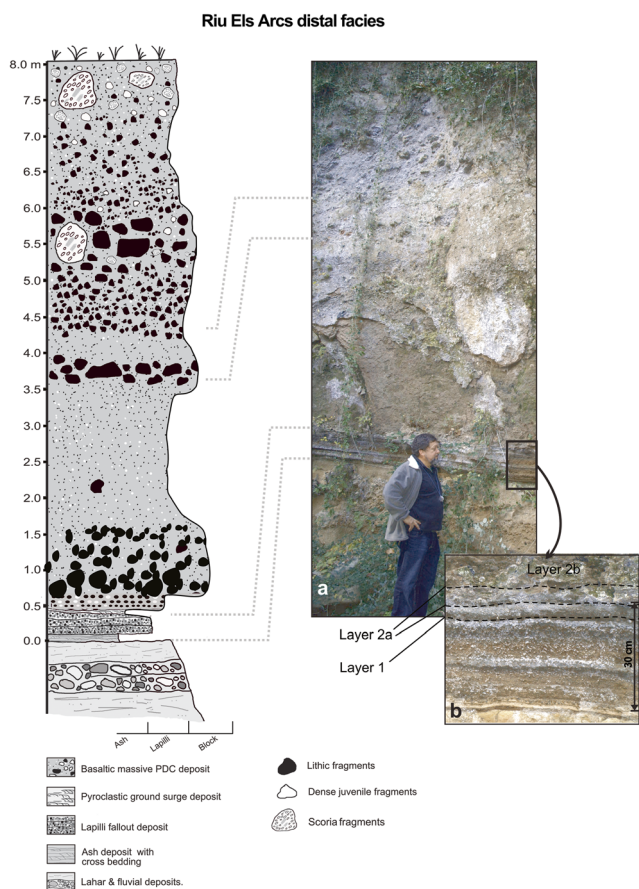
Fig. 5 Riu dels Arcs distal stratigraphic succession (see Fig. 2 point 3 for location) (UTM 31N—ETRS89 465883.0 and 4664738.2) with a more stratified and internally organised massive PDC deposit. **a** General view of the succession. **b** Close-up view of the lower part of the deposit in which layers 1 and 2a are visible

and has an estimated maximum thickness of about 25 m. During its emplacement, this deposit completely filled the gully but has been subsequently eroded. Today, the deep walls of the gully provide impressive outcrops of this massive PDC deposit.

In proximal areas (Canet d'Adri village, point 4 in Fig. 2), there is a stratified, brown, massive PDC deposit, about 12–15 m thick (Fig. Fig. 6). This deposit is composed of five depositional units, each several metres thick, which contain similar components but variable matrix-clast ratios and grain-size distributions. These units are separated by planar shear contacts that can be traced through the whole outcrop. There is no evidence for any time lapse (i.e. palaeosoils, erosion surfaces, alteration surfaces, etc.) between the units and all are assumed to have been deposited by different pulses of the same eruptive episode (Pedrazzi et al. 2016). The whole deposit has crude vertical columnar jointing that has produced individual hexagonal columns 2–5 m in diameter. The lower unit is very lithic-rich, with clasts of Eocene limestones, red sandstone and older grey lavas, some up to 1 m in diameter, embedded in a highly indurated ashy-to-fine lapilli matrix that
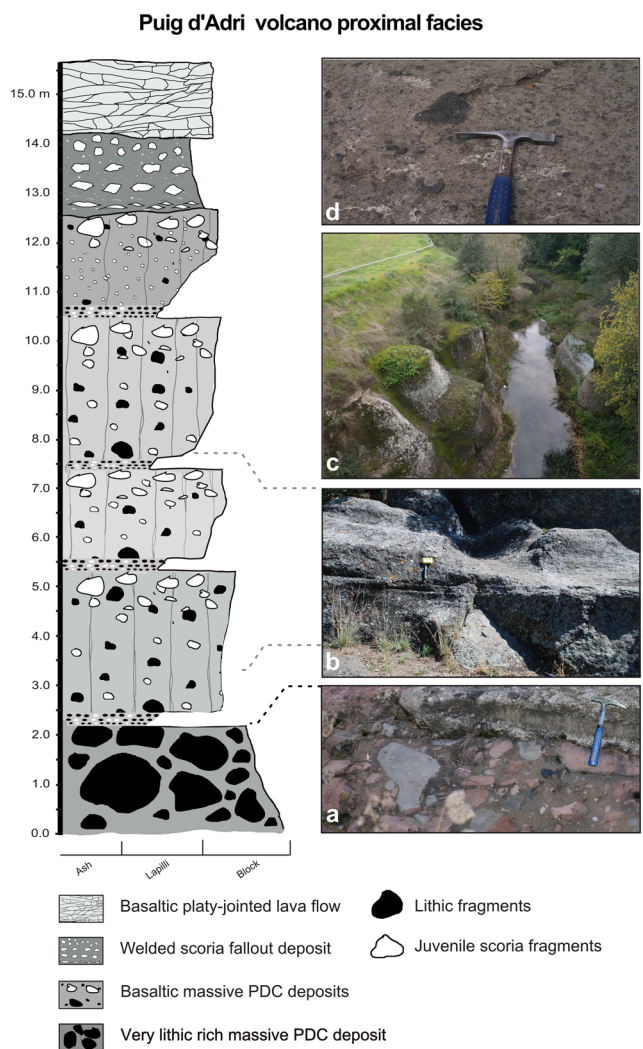
Fig. 6 Puig d'Adri proximal stratigraphic succession (Canet d'Adri, see Fig. 2 point 4 for location) (UTM 31N—ETRS89 477659.3 and 4653835.4). In this locality, the massive PDC deposit includes different depositional units with a very similar internal structure composed of layers 2a and 2b, along with a very lithic-rich unit at the base. **a** Detail of the very lithic rich unit. **b** Two successive depositional units in the massive PDC deposit separated by a planar contact. **c** Detail of the massive PDC deposit from above in which it is possible to observe individual columns resulting from differential erosion through columnar jointing. **d** Close-up view of one of the depositional units with juvenile scoria fragments (*black*) and lithic clasts (*red* and *grey*)
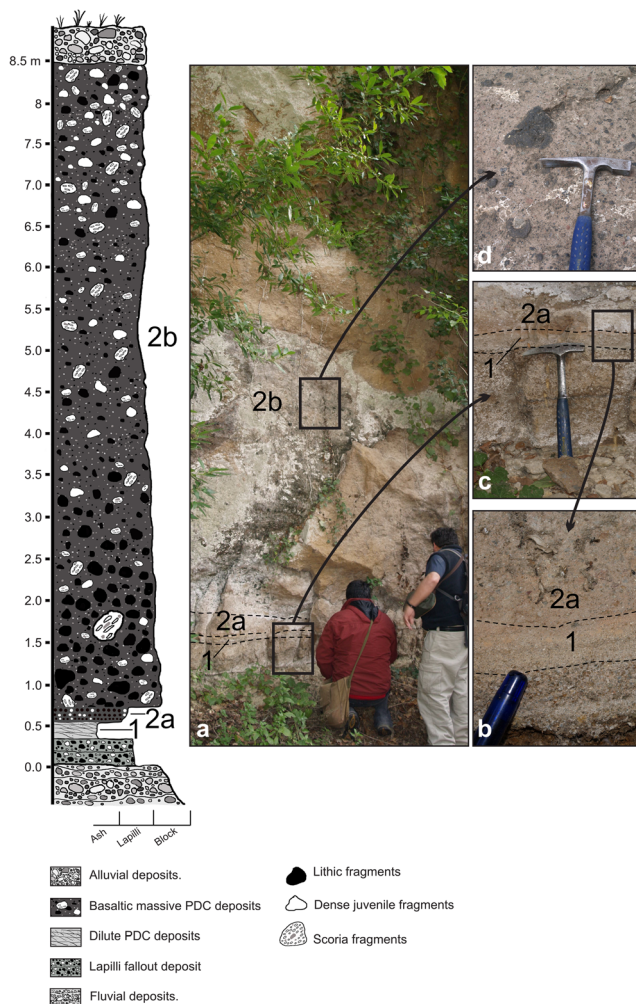
is very similar in composition and texture to the matrices described in the previous deposits. The next three units consist of massive deposits with poorly-to-highly vesiculated scoria fragments, up to a few decimetres in size, and cauliflower bombs in an abundant, fine-grained brown matrix composed of the same type of accidental lithic clasts as the lower unit and poorly-to-highly vesiculated juvenile clasts. Some scoria clasts exhibit peridotite enclaves. Although the lithic clasts tend to be coarse, tail normally graded, the largest juvenile fragments show reverse coarse-tail grading. The uppermost unit is lithic-poor with relatively more finer-grained scoria.

The base of each unit is composed of a few-centimetres-thick fine ash-rich horizon that gradually merges into the massive unit. The top of this massive PDC deposit is unconformably overlain by a welded scoria fallout deposit. In this unit, juvenile fragments are equant at the top but are fiamme-shaped at the base. The whole unit is covered by a black, platy-jointed basaltic lava flow.

About 5 km from the vent, at Molí de Can Cadamont (Fig. Fig. 7 and point 5 in Fig. 2), this massive deposit is exposed along the Canet river, where it overlies earlier pyroclastic deposits from the same eruption (Pedrazzi et al. 2016). Here, unconformably overlying older fluvial deposits, are two beds of lapilli fallout composed of black scoria and some dense juvenile fragments, and each bed is ~15 cm thick, with no clear gradation in grain size. An erosional contact separates this fallout deposit from a 30-cm-thick cross-bedded PDC

Puig d'Adri volcano distal facies

Fig. 7 Puig d'Adri (Molí de Can Cadamont) distal stratigraphic succession (see Fig. 2 point 5 for location) (UTM 31N—ETRS89 478662.8 and 4651992.9). Outcrop view (a). Details of layer 1 (ground surge) (b), layer 2a (c) and layer 2b (d)

deposit, which is composed of fine-lapilli-to-coarse-ash scoria. Concordant with this deposit, there is an 8-m-thick massive, brown matrix-supported deposit, containing clasts up to 5 cm in diameter (but mostly less than 2 cm) of black scoria and dense black juvenile material. The latter contain olivine and plagioclase phenocrysts. Also present are Eocene red sandstone, limestone and schist lithic clasts, all less than 2 cm in diameter. These lithic clasts are more abundant towards the lower half of the deposit, while scoria fragments are more abundant in the upper half. The matrix is formed of ash and fine lapilli scoria and is in general weathered and indurated, with zeolites, carbonates and iron oxide minerals precipitated in pore space. The deposit has an irregular eroded top surface and is covered by fluvial deposits. Compared to the proximal locality (Canet d'Adri), this deposit here is more homogeneous in texture and grain size in its distal part, and there is no evidence of the depositional units that constitute it closer to the vent. Additionally, there is no columnar jointing in distal parts. However, the deposit does have a layer of fine ash at its base that resembles that seen in the proximal locality and in the other massive PDC deposits described in this study. At the base, there is a diffuse planar contact with the cross-bedded PDC deposit that towards the top grades into the massive unit. The total thickness of this fine-grained layer is about 20 cm.

Discussion

The products of monogenetic basaltic volcanism range from lava flows and proximal fire-fountaining-derived fallout deposits in less explosive Hawaiian and Strombolian eruptions to distal tephra deposits and a wide range of PDC deposits in highly explosive eruptions in which magma/water interact (Connor and Conway 2000; Walker 2000; Valentine and Gregg 2008; Németh and Keretzturi 2015). The PDC deposits described in monogenetic volcanism mostly include those originated from dilute and highly expanded PDCs derived from ash-laden eruption columns and laterally directed explosions to wet jetting and continuous up rush of water-pyroclast slurries (Wohletz and Sheridan 1983; Sheridan and Wohletz 1981; Cas and Wright 1987; Valentine and Gregg 2008; Németh and Keretzturi 2015). Massive debris flow deposits and lahars have also been reported in association with monogenetic volcanism (Lorenz 1986; Németh and White 2003).

Massive PDC deposits similar to the ones described in this study have been reported in other monogenetic volcanic fields (e.g. White 1991; Valentine et al. 2000; Giordano et al. 2002; Brand and Clarke 2009; Brand et al. 2009; van Otterloo et al. 2013; van Otterloo and Cas 2016) and have been invariably interpreted as resulting from the emplacement of high-density PDCs. These massive PDC deposits resemble the classical small-volume ignimbrites that derive from explosive

eruptions of silicic magmas (see Sparks et al. 1973), and their eruption, transport and emplacement mechanisms may be interpreted in the same way. Ignimbrite deposits are not exclusive to silicic volcanism and have also formed during mafic eruptions of central or composite volcanoes (e.g. Freundt and Schmincke 1995; De Rita et al. 2002; Miyabuchi et al. 2006); nonetheless, such deposits are rare in monogenetic basaltic volcanism (see White 1991; Giordano et al. 2002; van Otterloo et al. 2013; van Otterloo and Cas 2016). Also, Gernon et al. (2009) and Fontana et al. (2011) described several examples of thick, massive, unambiguous PDC deposits at kimberlite volcanoes in southern Africa.

Several characteristics of the studied deposits from the GVZ are similar to typical low-to-medium-volume silicic ignimbrites emplaced by PDCs generated by the fountaining of vertical eruption columns (see Sparks et al. 1973); these include (i) presence of a dilute PDC deposit at the base of the massive deposits; (ii) presence of a fine-grained layer forming the lower part of the massive unit; (iii) occasional presence of a lithic-rich layer above the fine-grained layer; (iv) normal coarse-tail grading of the dense lithic clasts; (v) reverse coarse-tail grading of the less dense scoria clasts; (vi) grain-size distribution; (vii) evidence of partial welding and (viii) columnar jointing.

Since the seminal study of Sparks et al. (1973), a considerable body of work, covering field studies, numerical studies and laboratory experiments, has been done (e.g. Valentine and Wohletz 1989; Branney and Kokelaar 1992; Druitt 1998; Burgisser and Bergantz 2002; Sulpizio and Dellino 2008; Roche 2012, 2015; Dufek et al. 2015; Dufek 2016; Roche et al. 2016). Some of these studies directly contradict and negate some of the central interpretations of the Sparks et al. (1973) model and must be taken into account when trying to interpret similar deposits. However, it is remarkable how similar in terms of lithofacies and depositional sequences are the deposits studied here compared to those described by Sparks et al. (1973). This suggests that regardless of whether or not the interpretations provided by these authors were correct, both types of deposits, despite deriving from contrasting magma compositions, share common eruption, transport and depositional mechanisms and, consequently, have similar hazard implications.

The fine-grained, thinly laminated and cross-bedded PDC deposits that precede the emplacement of the massive PDC deposits in the three examples studied seem to correspond to ground surge deposits (Layer 1 in Sparks et al. 1973) laid beneath the front of the PDC due to the intense interaction between the PDC and the ground surface (Sparks and Walker 1973; Wilson and Walker 1982; Valentine and Fisher 1986; Freundt et al. 2000). Accordingly, the massive PDC deposit units would correspond to layer 2 sensu Sparks et al. (1973). In all three cases, there is a reverse-graded ash layer at the base that can be interpreted either as the product of the interaction

(friction) between the main flow and the substratum or as a fine-grained deposit sedimented from the front of the flow. This fine-grained layer that can be compared to layer 2a of Sparks et al. (1973) grades into the main body of the deposit; although at some points, the contact between the two is more abrupt. The main part of the deposit (layer 2b, Sparks et al. 1973) is massive in all cases but characterised by normal-to-coarse tail-grading in the lithic clasts and reverse grading in the lighter juvenile fragments. The fine ash layer (layer 3) described by Sparks et al. (1973) is not evident on top of the GVF massive deposits, probably due to post-depositional erosion.

Due to their high degree of induration, it was not possible to conduct any grain-size analysis of these deposits using sieving techniques. However, an estimate of the grain-size distribution estimate was carried out using macroscopic and microscopic image analysis. This reveals that these deposits have a polymodal grain-size distribution frequency with high sorting coefficients (>2), as is characteristic in classical ignimbrites (Sparks et al. 1973; Sparks 1976; Freundt et al. 2000; Sulpizio and Dellino 2008; Dufek et al. 2015; Dufek 2016). The ash-grade matrix (15–40% in volume) is invariably composed of devitrified glass shards and small scoria fragments and maintains in all cases a variable proportion of lithic clasts (15–40% in volume), as well as dense (10–30% in volume) or vesiculated (5–15%) juvenile scoria fragments. The most abundant of these generally angular-to-sub-rounded lithic clasts are those derived from Eocene red sandstones (up to 80% of the total), followed by old lavas and subordinate Eocene limestones. Some juvenile clasts show rounded-to-sub-rounded morphologies, which is probably evidence of abrasion during transport. There is also evidence in these deposits of a relatively high emplacement temperature, despite the fact that their high lithic content should theoretically result in a significant decrease in the initial flow temperature during emplacement (see Martí et al. 1991). The presence of flattened scoria clasts and columnar jointing are evidence of high emplacement temperatures (e.g. Freundt et al. 2000). However, even though the original vitroclastic textures are still recognisable, the degree of alteration of the matrix means that it is unclear if the matrix ash shards are welded. Even so, the application of a progressive thermal demagnetization procedure to these pyroclastic deposits (Parés et al. 1993) revealed stable magnetizations up to about 590 °C and no thermally induced mineralogical changes below 620 °C, which suggests that the maximum emplacement temperature of the Eocene red sandstones in these deposits was ~580 °C. This result, together with the fact that a temperature over 400 °C is required to unblock the TRM of magnetite (as revealed by the demagnetization during the laboratory-induced TRM), suggests that the emplacement temperature of these deposits would probably have been around 450–500 °C: the temperature at which magnetite appears at the expense of hematite in these Tertiary red sandstones (Parés et al. 1993). Assuming an

initial temperature of the basaltic magma of 1200 °C, the decrease in temperature in these pyroclastic flows during emplacement was about 700 °C.

All the studied deposits show valley-fill cross-sectional patterns, which suggests emplacement by dense, high-particle concentration, gas-lubricated particulate flows (see Sparks et al. 1973: Wilson and Walker 1982; Druitt 1998; Freundt et al. 2000; Sulpizio and Dellino 2008; Roche 2012; Dufek et al. 2015; Dufek 2016). The characteristics of the studied deposits (matrix-supported textures, and coarse-tail grading) indicate that turbulence was suppressed by high particle concentrations, thus enhancing differences in the settling velocities of the different clasts during the transport of the main flow body. However, the presence of localised thin cross-bedded deposits at the base of the massive deposits and the discontinuous or lenticular morphology of this layer throughout the entire lateral extent of the parent dense PDC also indicates localised turbulent interaction between the PDCs and topography (Valentine and Fisher 1986). Entrainment of a significant volume of atmospheric air into the pyroclastic flow and its further expansion would have contributed to reducing its initial temperature together with the incorporation of cold lithic clasts from the conduit. The presence of lenses of lithic clasts and fine-depleted zones would also provide evidence for periodic turbulent transport in the lower flow boundary zone in contact with the substrate. Above the zone, the PDC would be entirely turbulent all the time. However, it is impossible to provide any estimate of the volumetric expansion of these pyroclastic flows during emplacement, as any possible fine-grained deposits derived from an overlying turbulent ash cloud on top of the massive deposits (layer 3 of Sparks et al. 1973) or as veneer or overbank deposits will have been removed by subsequent erosion.

Pyroclastic density currents generated during explosive volcanism may exhibit emplacement velocities from a few m/s to well over 100 m/s and may travel tens of kilometres or more from the vent depending on their eruption dynamics and flow characteristics (Sparks et al. 1978; Valentine and Wohletz 1989). In the case of the small-volume massive PDC deposits in the GVF, the maximum observed run-out distances are 6–7 km. The minimum emplacement velocities likely for these flows can be estimated at about 4.41 to 6.76 m/s (15.87 to 24.34 km h^{-1}) using the approaches of Pittari et al. (2007) and Roche (2015), respectively (see Appendix 1), which correspond to typical values for PDCs of similar characteristics (see Roche 2015)

Therefore, the characteristics of the massive PDC deposits studied here suggest that they were formed by deposition from high-particle-concentration PDCs that behaved in a similar way to the low-to-intermediate volume, pumice-rich PDCs that are responsible for the deposition

of silicic ignimbrites. Given these transport and depositional characteristics, these deposits cannot be the product of resedimentation processes, syn-eruptive debris flows or lahars. The eruption mechanisms responsible for the generation of such PDCs can be explained within the framework of the phreatomagmatic activity that characterised these eruptions. In fact, the presence of abundant lithic fragments from the Eocene aquifer that underlies the whole area at a depth of 200–300 m is clearly indicative of the occurrence of a magma/water interaction during the eruptions. In addition, the presence of poorly (dense) vesiculated scoria juvenile clasts in all deposits (which are occasionally preceded and succeeded by deposits from dilute PDCs) are further clear indicators of a magma/water interaction. However, it should be noted that these deposits have only ever been found in eruptions where explosivity occurred in the Eocene aquifer. Other phreatomagmatic eruptions in the same area (e.g. Croscat, Sant Dalmai), caused by an interaction between magma and water in the shallower Quaternary aquifer, produced only dilute PDC deposits (Martí et al. 2011). This suggests that the conditions for generating massive flows are only achieved when the magma/water interaction is controlled by the hydraulic conditions and depth of the Eocene aquifer, which is characterised by its relatively low transmissivity (25 m^2/day), a total depth of 400 m and a non-saturated zone of 10 m (Joan Bach, personal communication). We infer that the flows were formed by the almost immediate collapse of short but dense eruption columns resulting from a high discharge rate that were produced during large energetic Vulcanian or phreato-Vulcanian explosive events (Fig. Fig. 8), similar to the process described by van Otterloo et al. (2013) and van Otterloo and Cas (2016). The presence of several flow units in some cases, however, indicates that several explosions may have occurred during the same eruptive phase, thereby generating subsequent flow pulses that were superimposed following very similar flow dynamics to those of silicic ignimbrites.

We thus propose that these massive PDC deposits or ignimbrites were the product of transient explosions when groundwater came into contact with magma during steady phases of Strombolian eruptions. The presence of well-stratified scoria lapilli fall deposits at the base of most of these ignimbrites indicates that their emplacement was preceded by a sustained high-fire-fountaining/short eruption column phase during a Strombolian eruption. Massive disruption of the underground water in the confined Eocene aquifer, probably due to a decrease in the pressure inside the conduit, caused a drastic change in the eruption dynamics, giving rise to a sudden increase in the explosivity at depth. This led to the erosion of the conduit and, subsequently, an increase in the mass eruption rate, thereby overloading the eruption column and causing it to collapse
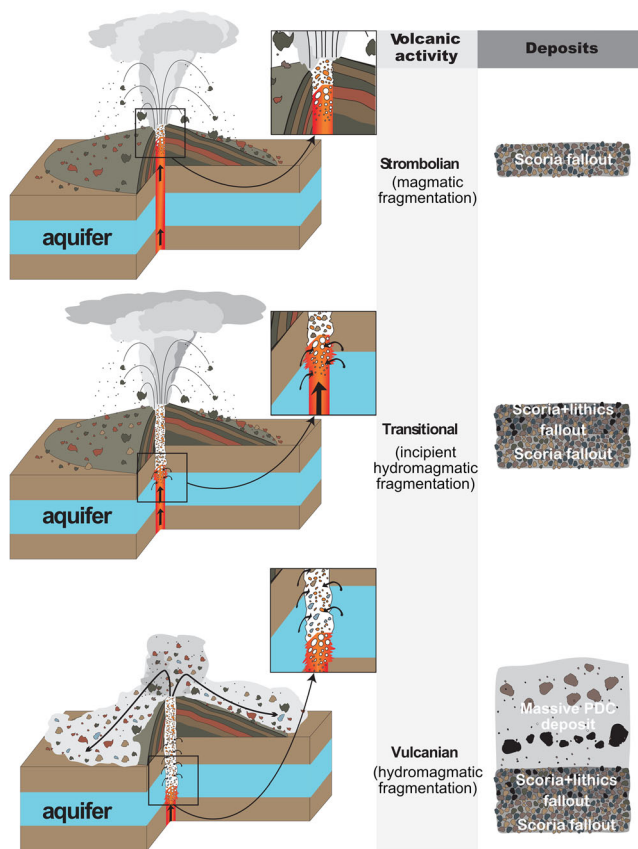
Fig. 8 Interpretative sketch of the eruption mechanisms that generated the basaltic ignimbrites in La Garrotxa Volcanic Zone. In all cases of ignimbrite deposits observed in the GVF, the succession of deposits is very similar, which suggest a common eruption mechanism for all of them. These eruption phases were preceded by pure Strombolian magmatic episodes, characterised by magmatic fragmentation and formation of scoria fallout deposits. Progressively magma/water (from the Eocene aquifer) interaction started giving rise to the initiation of hydromagmatic fragmentation and the incorporation of lithic clasts from the Eocene aquifer in the scoria deposit. The phreatomagmatic character of the eruption suddenly increased due to a more effective magma/water interaction, generating vulcanian explosions that gave rise to the formation of overloaded eruption columns, rich in scoria fragments and lithic clasts from the Eocene aquifer and the substrate rocks above it. These eruption columns collapsed very rapidly, forming dense PDCs mostly emplaced down the main valleys and gullies. The transport and deposition of these dense basaltic PDCs occurred in a similar way as some small-volume silicic ignimbrites, giving rise to the same facie association as that first described by Sparks et al. (1973) (see text for further explanation)

over the crater and generate the PDC. The lack of compositional and textural changes of magma during these eruptions and the systematic appearance of Eocene lithic clasts in the transition from Strombolian to phreatomagmatic phases do not support the possible effect of variable gas content, transient blocking of the conduit or groundmass crystallisation in the magma as causes for the increased explosivity. The resulting flows were emplaced into topographic depressions as highly concentrated PDCs that were deposited up to several kilometres away as high-density,

granular flows (cf. Roche 2012) when the initial momentum dissipated. On some occasions (e.g. Puig d'Adri), the transient explosions were repeated several times during the eruption and generated several flow units that produced tens-of-metres-thick composite succession.

In addition to the three deposits we have described in detail here, we know of the presence of many more in the GVF. Similar dense-PDC deposits have been described in other volcanic fields (e.g. White 1991; Giordano et al. 2002; Gernon et al. 2009; van Otterloo et al. 2013), which suggests that, in addition to the more common dilute PDCs, the formation of this particular type of dense PDC may also occur when magma/water interact in confined aquifers with relatively low transmissivity located a few hundred meters below the surface. This is thus a reminder of the importance in hazard assessment of understanding the characteristics of the substrate in volcanic fields and, in particular, of the aquifers that may exist at relatively shallow depths since they could have an unexpected—and thus serious—impact at considerable distances from the vent.

Conclusions

The lithological and sedimentological characteristics of some of the massive basaltic PDC deposits in La Garrotxa Volcanic Field are similar to those of low-to-intermediate-volume ignimbrites generated during explosive eruptions of silicic magmas. We infer that these basaltic ignimbrites were derived from transient phreatomagmatic episodes occurring during Strombolian eruptions whose dynamics suddenly changed and gave rise to a substantial increase in their explosivity and mass flow rate. This generated overloaded eruption columns that immediately collapsed, forming the flows that emplaced chiefly along the main valleys and gullies. These pyroclastic flows achieved velocities of several metres per second, with run-out distances of up to 6 km from the vent, and were deposited at relatively high temperatures (up to 550 °C). The fact that the resulting deposits present very similar features to medium-to-low-volume silicic ignimbrites implies that despite the differences between their eruptions dynamics and nature of juvenile components, the transport and depositional mechanisms in both types of volcanic processes were similar. Eruptions with these dynamics and capable of producing such deposits thus represent an inherent and significant hazard in monogenetic basaltic volcanism, which is traditionally assumed to represent only a low threat.

Appendix 1

Approximate minimum flow velocities have been calculated using the approaches proposed by Pittari et al. (2007) and Roche (2015), both aimed at calculating the minimum flow velocity required by the parent flow to move lithic clasts captured from an underlaying substrate to a certain distance. Following Pittari et al. (2007), if we assume that the force required to move a static clast of certain dimension and density resting on bedrock is

$$F1 = u_s mg \qquad (1)$$

and that the force applied to a clast at rest by a pyroclastic flow is

$$F2 = 0.5 \rho_{fl} v^2 C_D A \qquad (2)$$

where u_s is the coefficient of static friction, m is the clast mass, g is the acceleration due to gravity, ρ_{fl} is the bulk density of the pyroclastic flow, v is the pyroclastic flow velocity, C_D is the coefficient of aerodynamic drag and A is the clast surface impacted by the flow force, and making $F1 = F2$, we have that

$$v^2 = u_s mg / 0.5 \rho_{fl} C_D A \qquad (3)$$

Considering a lithic clast size dimensions of $0.8 \times 0.5 \times 0.3$ (volume $= 0.12$ m^3), which corresponds to the maximum lithic clast (Eocene feldspathic sandstone) size we have recorded, and the following input values: $u_s = 0.7$; $A = 0.15$ m^2; $m = 300$ kg (clast density $= 2500$ kg/m^3); $g = 10$ ms^{-2}; $\rho_{fl} = 1800$ kg/m^3; $C_D = 0.8$, we obtain $v = 4.41$ m/s (15.87 km/h). If we used the equation proposed by Roche (2015)

$$v^2 = \left(\rho_p - \rho_f \right) gC \div \gamma \rho \qquad (4)$$

where ξ, is a shape factor equal to 2.3 for an ellipsoid, ρ_p is the clast density, ρ_f is the gas density ($\sim$1 kg/m^3), g is the acceleration of gravity, C is the short length of the clast, $\gamma \approx 0.06$ is an empirical factor and ρ is the bulk flow density, and using the same input values that in the previous case, we obtain a minimum flow velocity of 7 m/s, equivalent to 24 km/h.

References

Araña V, Aparicio A, Martín-Escorza C, García Cacho L, Ortiz R, Vaquer R, Barberi F, Ferrara G, Albert J, Gassiot X (1983) El volcanismo Neógeno-Cuaternario de Catalunya: carácteres estructurales, petrológicos y geodinámicos. Acta Geol Hisp 18:1–17

Blong RJ (1984) Volcanic hazards: a sourcebook on the effects of volcanic eruptions. Academic Press, Sidney

Blong RJ (2000) Volcanic hazards and risk management. In: Sigurdsson H, Houghton B, Rymer H, Stix J, McNutt S (eds) Encyclopedia of volcanoes. Academic Press, San Diego, pp 1215–1227

Bolós X, Planagumà L, Martí J (2014) Volcanic stratigraphy and evolution of the Quaternary monogenetic volcanism in the Catalan volcanic zone (NE Spain). J Quat Sci 29(6):547–560

Bolós X, Martí J, Becerril L, Planagumà L, Grosse P, Barde-Cabusson S (2015) Volcano-structural analysis of la Garrotxa volcanic field (NE Iberia): implications for the plumbing system. Tectonophysics 642: 58–70. doi:10.1016/j.tecto.2014.12.013

Brand BD, Clarke AB (2009) The architecture, eruptive history, and evolution of the table rock complex, Oregon: from a Surtseyan to an energetic maar eruption. J Volcanol Geotherm Res 180:203–224

Brand BD, Clarke AB, Semken S (2009) Eruptive conditions and depositional processes of Narbona Pass Maar volcano, Navajo volcanic field, Navajo nation, New Mexico (USA). Bull Volcanol 71:49–77. doi:10.1007/s00445-008-0209-y

Branney MJ, Kokelaar P (1992) A re-appraisal of ignimbrite emplacement: progressive aggradation and changes from particulate to non-particulate flow during emplacement of high-grade ignimbrite. Bull Volcanol 54:504–520

Branney MJ Kokelaar P (2002) Pyroclastic density currents and the sedimentation of ignimbrites. Geol Soc London, Geol Soc Mem n 27, 143 pp

Burgisser A, Bergantz GW (2002) Reconciling pyroclastic flow and surge: the multiphase physics of pyroclastic density currents. Earth Planet Sci Lett 202:405–418

Cas RAF, Wright JV (1987) Volcanic succession modern and ancient—a geological approach to processes, products and successions. Allen & Unwin, London **487 pp**

Cebriá JM, López-Ruiz J, Doblas M, Oyarzun R, Hertogen J, Benito R (2000) Geochemistry of the Quaternary alkali basalts of Garrotxa (NE Volcanic Province, Spain): a case of double enrichment of the mantle lithosphere. J Volcanol Geotherm Res 112:175–187

Cimarelli C, Di Tragia F, de Rita D, Gimeno Torrente D, Fernandez Turiel JL (2013) Space–time evolution of monogenetic volcanism in the mafic Garrotxa volcanic field (NE Iberian peninsula). Bull Volcanol 75:758

Connor CB, Conway FM (2000) Basaltic volcanic fields. In: Sigurdsson H (ed) Encyclopedia of volcanoes. Academic Press, San Francisco (CA), pp 331–343

De Rita D, Giordano G, Esposito A, Fabbri M, Rodani S (2002) Large volume phreatomagmatic ignimbrites from the Colli Albani volcano (middle Pleistocene, Italy). J Volcanol Geotherm Res 118:77–98

Druitt T (1998) Pyroclastic density currents. Geol Soc Lon Spec Public 145:145–182. doi:10.1144/GSL.SP.1996.145.01.08

Dufek J (2016) The fluid mechanics of pyroclastic density currents. An Rev Fluid Mech 48:459–485. doi:10.1146/annurev-fluid-122414-034252

Dufek J, Ongaro TE, Roche O (2015) Chapter 15: pyroclastic density currents: processes and models, in The Encyclopedia of Volcanoes. Copyright Elsevier Inc, 617–629. doi: 10.1016/B978-0-12-385938-9.00035-3

Fontana G, Mac Niocaill C, Brown RJ, Sparks RSJ, Field M (2011) Emplacement temperatures of pyroclastic and volcaniclastic deposits in kimberlite pipes in southern Africa. Bull Volcanol 73(8): 1063–1083

Freundt A, Schmincke HU (1995) Eruption and emplacement of a basaltic welded ignimbrite during caldera formation on Gran Canaria. Bull Volcanol 56:640–659

Freundt A, Wilson CJN, Carey SN (2000) Ignimbrites and block and ash flow deposits. In: Sigurdsson H, Houghton B, Rymer H, Stix J, McNutt S (eds) Encyclopedia of volcanoes. Academic Press, San Francisco (CA), pp 581-600

Gernon TM, Fontana G, Field M, Sparks RSJ, Brown RJ, Mac Niocaill C (2009) Pyroclastic flow deposits from a kimberlite eruption: the Orapa south crater, Botswana. Lithos 112:566–578

Giordano G, De Rita D, Cas R, Rodani S (2002) Valley pond and ignimbrite veneer deposits in the small-volume phreatomagmatic

'Peperino Albano' basic ignimbrite, Lago Albano maar, Colli Albani volcano, Italy: influence of topography. J Volcanol Geotherm Res 118:131–144

Gisbert G, Gimeno D, Fernández-Turiel JL (2009) Eruptive mechanisms of the Puig De La Garrinada volcano (Olot, Garrotxa volcanic field, northeastern Spain): a methodological study based on proximal pyroclastic deposits. J Volcanol Geotherm Res 180:259–276

López Ruiz J, Rodriguez Badiola E (1985) La región volcánica Mio-Pleistocena del NE de España. Estud Geol 41:105–126

Lorenz W (1986) On the growth of maars and diatremes and its relevance to the formation of tuff rings. Bull Volcanol 48:265–274

Lowe DR (1979) Sediment gravity flows: their classification and some problems of application to natural flows and deposits. SEPM (Spec Public 27), pp 75–82

Lowe DR (1982) Sediment gravity flows: II depositional models with special reference to the deposits of high-density turbidity currents. J Sediment Petrol 52:279–297

Martí J, Mallarach JM (1987) Erupciones hidromagmáticas en el volcanismo cuaternario de Olot (Girona). Estud Geol 43:31–40

Martí J, Diez-Gil JL, Ortiz R (1991) Conduction model for the thermal influence of lithic clasts in mixtures of hot gases and ejecta. J Geophys Res 96:1,879–21,885

Martí J, Mitjavila J, Roca E, Aparicio A (1992) Cenozoic magmatism of the Valencia trough (western Mediterranean): relation between structural evolution and volcanism. Tectonophysics 203:145–166

Martí J, Planagumà L, Geyer A, Canal E, Pedrazzi D (2011) Complex interaction between Strombolian and phreatomagmatic eruptions in the Quaternary monogenetic volcanism of the Catalan volcanic zone (NE of Spain). J Volcanol Geotherm Res 201:178–193

Middleton GV (1993) Sediment deposition from turbidity currents. Annu Rev Earth Planet Sci 21:89–114

Middleton GV, Hampton MA (1973) Sediment gravity flows: mechanics of flow and deposition. In: Middleton GV, Bouma AH (eds) Turbidites and deep water sedimentation. SEPM, Anaheim **Short Course Notes, 38p**

Miyabuchi Y, Watanabe K, Egawa Y (2006) Bomb-rich basaltic pyroclastic flow deposit from Nakadake, Aso volcano, southwestern Japan. J Volcanol Geotherm Res 155:90–103

Németh K, Keretzturi G (2015) Monogenetic volcanism: personal views and discussion. Int J Earth Sci 104:2131–2146

Németh K, White JDL (2003) Reconstructing eruption processes of a Miocene monogenetic volcanic Åëeld from vent remnants: Waipiata volcanic field, South Island, New Zealand. J Volcanol Geotherm Res 124:1–21

Neumann ER, Martí J, Mitjavila J, Wulff-Pedersen E (1999) Origin and implications of mafic xenoliths associated with Cenozoic extension-related volcanism in the València Trough, NE Spain. Mineral Petrol 65:113–139

van Otterloo J, Cas RAF (2016) Low-temperature emplacement of phreatomagmatic pyroclastic flow deposits from maar craters at the monogenetic Mt Gambier volcanic complex, South Australia, and their relevance for understanding some deposits in maar diatreme fills. J Geol Soc. doi:10.1144/jgs2015-122

van Otterloo J, Cas RAF, Sheard MJ (2013) Eruption processes and deposit characteristics at the monogenetic Mt. Gambier volcanic complex, SE Australia: implications for alternating magmatic and phreatomagmatic activity. D Bull Volcanol 75:737. doi:10.1007/s00445-013-0737-y

Parés JM, Martí J, Garcés M (1993) Thermoremanence in red sandstone clasts and emplacement temperature of a Quaternary pyroclastic deposit (Catalan volcanic zone, NE Spain). Stud Geophys Geod, Special Issue on "New Trends in Geomagnetism" 37:401–414

Pedrazzi D, Bolós X, Martí J (2014) Phreatomagmatic volcanism in complex hydrogeological environments: La Crosa de Sant Dalmai maar (Catalan Volcanic Zone, NE Spain). Geosphere. doi:10.1130/ges00959.1

Pedrazzi D, Bolós X, Barde-Cabusson S, Martí J (2016) Reconstructing the eruptive history of a monogenetic volcano through a combination of fieldwork and geophysical surveys: the example of Puig d'Adri (Garrotxa volcanic field). Jour Geol Soc. doi:10.1144/jgs2016-009

Pittari A, Cas RAF, Monaghan J, Marti J (2007) Instantaneous dynamic pressure effects on the behaviour of lithic boulders in pyroclastic flows: the Abrigo ignimbrite, Tenerife, Canary Islands. Bull Volcanol 69:265–279

Roche O (2012) Depositional processes and gas pore pressure in pyroclastic flows: an experimental perspective. Bull Volcanol 74:1807–1820. doi:10.1007/s00445-012-0639-4

Roche O (2015) Nature and velocity of pyroclastic density currents inferred from models of entrainment of substrate lithic clasts. Earth Planet Sci Lett 418:115–125

Roche O, Buesch DC, Valentine GA (2016) Slow-moving and far-travelled dense pyroclastic flows during the Peach Spring super-eruption. Nature Commun 7:10890 doi:10.1038/ncomms10890

Sheridan MF, Wohletz KH (1981) Hydrovolcanic explosions: the systematics of water-pyroclast equilibrium. Science 212:1387–1389

Sparks RSJ (1976) Grain size variations in ignimbrites and implications for transport of pyroclastic flows. Sedimentology 23:147–188

Sparks RSJ, Walker GPL (1973) The ground surge deposit: a third type of pyroclastic rock. Nature 241:62–64

Sparks RSJ, Self S, Walker GPL (1973) Products of ignimbrite eruptions. Geology 1:115–118

Sparks RSJ, Wilson L, Hulme G (1978) Theoretical modeling of the generation, movement and emplacement of pyroclastic flows by column collapse. J Geophys Res 83:1727–1739

Sulpizio R, Dellino P (2008) Chapter 2 sedimentology, depositional mechanisms and pulsating behaviour of pyroclastic density currents. In: Gottsmann JH, Martí J (eds) Developments in volcanology, caldera volcanism: analysis, modelling and response, vol 10, pp 57–96

Tilling RI (1989) Volcanic hazards and their mitigation: progress and problems. Rev Geophys 27:237–269

Tilling RI (2005) Volcano hazards, in Martí J and Ernst G (Edts): volcanoes and the environment. Cambridge University Press, Cambridge, pp 55–89

Valentine GA, Fisher RV (1986) Origin of layer 1 deposits in ignimbrites. Geology 14:146–148

Valentine GA, Gregg TKP (2008) Continental basaltic volcanism—process and problems. J Volcanol Geotherm Res 177:857–873

Valentine GA, Wohletz KH (1989) Environmental hazards of pyroclastic flows determined by numerical models. Geology 17:641–644

Valentine GA, Perry FV, Wolde Gabriel G (2000) Field characteristics of deposits from spatter-rich pyroclastic density currents at summer coon volcano, Colorado. J Volcanol Geotherm Res 104:187–199

Walker GPL (2000) Basaltic volcanoes and volcanic systems. In: In: Sigurdsson H, Houghton B, Rymer H, Stix J, McNutt S (eds) Encyclopedia of volcanoes. Academic Press, San Francisco (CA), pp 283–289

White JDL (1991) Maar–diatreme phreatomagmatism at Hopi buttes, Navajo nation (Arizona), USA. Bull Volcanol 53:239–258

White JDL, Schmincke H-U (1999) Phreatomagmatic eruptive and depositional processes during the 1949 eruption on La Palma (Canary Islands). J Volcanol Geotherm Res 94:283–304

Wilson CJN, Walker GPL (1982) Ignimbrite depositional facies: the anatomy of a pyroclastic flow. J Geol Soc Lon 139:581–592

Wilson L, Sparks RSJ, Walker GPL (1980) Explosive volcanic eruptions-IV: the control of magma properties and conduit geometry on eruption column behaviour. Geophys J R Astron Soc 63:117–148

Wohletz KM, Sheridan MF (1983) Hydrovolcanic explosions 2. Evolution of basaltic tuff rings and tuffs cones. Amer Jour Sci 283:385–413